THE JOURNAL OF PHYSICAL CHEMISTRY B

Article

pubs.acs.org/JPCB

Conjugated Polymer Nanoparticles Incorporating Antifade Additives for Improved Brightness and Photostability

Zhiyuan Tian,[†,‡] Jiangbo Yu,[†] Xiaoli Wang,[†] Louis C. Groff,[†] Jennifer L. Grimland,[†] and Jason D. McNeill*[,†]

[†]Department of Chemistry, Clemson University, Clemson, South Carolina 29634, United States

[‡]School of Chemistry and Chemical Engineering, University of Chinese Academy of Sciences (UCAS), Beijing 100049, P. R. China

Supporting Information

ABSTRACT: Conjugated polymer nanoparticles with incorporated antifade agents were prepared, and ensemble and single particle measurements showed that incorporation of antifade agents effectively improves the fluorescence quantum yield and photostability of the conjugated polymer nanoparticles, likely by a combination of triplet quenching and suppression of processes involved in photogeneration of hole polarons (cations), which act as fluorescence quenchers. The photostability of conjugated polymer nanoparticles and CdSe quantum dots was compared, at both the ensemble and single particle level. The results provide confirmation of the hypothesis that quenching by photogenerated hole polarons is a key factor limiting the fluorescence quantum yield and maximum emission rate in conjugated polymer nanoparticles. Additionally, the results indicate the involvement of oxygen in photogeneration of hole polarons. The results also provide insight into the origin of quenching processes that could limit the performance of conjugated polymer devices.

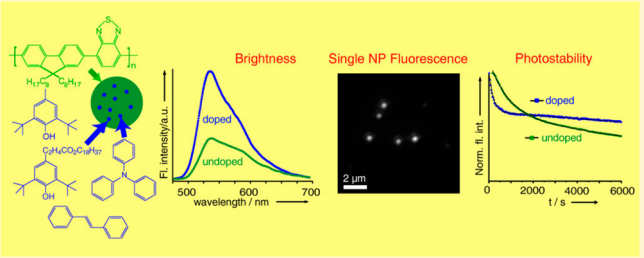

INTRODUCTION

Fluorescent conjugated polymer nanoparticles (CPNs) exhibit exceptional brightness and excellent photostability for photon-starved imaging applications such as video-rate and nanometer-resolution particle tracking.[1] Additionally, their high energy transfer efficiency is useful for several applications such as photoswitching nanoparticles,[2] single nanoparticle sensors,[3] and other advanced imaging and sensing applications.[4] While CPN brightness and photostability have been shown to rival or exceed those of other small (4−15 nm dia.) fluorescent nanoparticles,[5] additional improvements are sought in order to probe a wider array of processes in live cells and tissue and to improve spatial resolution and increase particle longevity in tracking experiments. The fluorescence brightness of a probe in a particular application depends on the optical absorption cross-section, fluorescence quantum yield, and photostability. The peak absorption cross sections of CPNs are roughly 3 orders of magnitude larger than typical organic fluorescent dyes and 10−100 times larger than typical CdSe quantum dots in the visible and near-UV.[6] However, the fluorescence quantum yields of CPNs are typically less than 40% and often less than 10%, leaving some room for improvement.[6]

Molecular oxygen is involved in a number of processes leading to photodegradation of organic dyes,[7] including formation of singlet oxygen, peroxides, and other reactive oxygen species (ROS). Triplet quenchers and ROS scavengers are often added as antifade agents, to reduce the rate of photobleaching in fluorescence microscopy of biological samples.[8] However, antifade agents are not typically used for live specimens, since they are cytotoxic or can perturb cell function at the high concentrations required (typically several weight percent). Photo-oxidation of polyfluorenes and related polymers has been observed to occur via multiple pathways, including formation of keto defects[9] and progressive oxidation of side chains that eventually results in oxidative damage to the conjugated backbone.[10] Furthermore, fluorescence photobleaching in conjugated polymers (and CPNs) can be greatly exacerbated by an indirect mechanism, in which photo-oxidized defects or photogenerated hole polarons act as highly efficient fluorescence quenchers.[6,11−13] For application of CPNs in fluorescence-based imaging or sensing applications, photobleaching involving oxygen is expected to be a critical problem, particularly for long-term imaging applications involving live cells and tissue. We report on a novel strategy for improving CPN photostability, by incorporating hydrophobic antifade agents in CPNs during nanoparticle formation. Ensemble (bulk) and single particle photobleaching measurements indicate that fluorescence fading is significantly reduced, by mechanisms including quenching of the relevant excited electronic states (e.g., triplet fluorophores and singlet oxygen), and scavenging of ROS. Some antifade agents are also observed to improve CPN fluorescence quantum yield, likely through

Special Issue: Paul F. Barbara Memorial Issue

Received: August 30, 2012
Revised: November 30, 2012
Published: December 6, 2012

suppression of reversibly photogenerated hole polarons. Additionally, the results provide a nanoscale, single-particle perspective on key device processes (e.g., electron transfer, photogeneration of polarons, and exciton quenching by polarons) in conjugated polymers.

EXPERIMENTAL METHODS

Conjugated polymer nanoparticles were prepared by reprecipitation induced by rapid addition of a solution of the polymer dissolved in tetrahydrofuran to deionized water, under sonication to induce rapid mixing, as described elsewhere.[14] Doped nanoparticles were prepared by coprecipitating from a solvent mixture containing equal amounts (1:1 weight ratio) of the polymer and one or more dopants. This ratio was chosen because it was determined that a weight ratio of roughly 1:1 yielded a significant improvement in photostability or fluorescence quantum yield (results provided below), whereas smaller amounts of the dopants (e.g, 10% relative to the polymer) yielded significantly reduced enhancements in photostability or fluorescence quantum yield (data not shown). Fluorescence quantum yields were determined by a combination of UV−vis and fluorescence spectroscopy using standard procedures. Particle diameters were determined by AFM measurements of particles cast on a glass substrate. Bulk fluorescence photobleaching kinetics measurements were obtained using 473-nm laser excitation, while a CCD spectrograph continuously acquired spectra. Single particle photostability measurements were performed using a fluorescence microscope with 473 nm laser excitation and EMCCD detector continuously acquiring images. A full description of materials, methods, and additional supporting data are provided in the Supporting Information.

RESULTS/DISCUSSION

We employed the conjugated polymer poly[(9,9-dioctylfluorenyl-2,7-diyl)-co-(1,4-benzo-{2,1′,3}-thiadiazole)] (PFBT) for the preparation of CPNs, owing to its excellent photostability and high brightness for laser-based fluorescence microscopy.[6] Four antifade agents (structures shown in Figure 1), butylated hydroxytoluene (BHT, an antioxidant and radical scavenger), 3-(3,5-ditert-butyl-4-hydroxyphenyl) propionic acid stearyl ester (PASE, a BHT derivative), triphenylamine (TPA, a singlet oxygen quencher), and *trans*-stilbene (TSB, a triplet quencher), were incorporated into PFBT nanoparticles during nanoparticle preparation by reprecipitation, yielding clear (not turbid), bright yellow nanoparticle dispersions, stable for weeks without aggregation.[14,15] A particle size distribution of ∼17 nm was determined by AFM for undoped PFBT particles as well as for particles codoped with TPA and TSB (Figure 1). Nanoparticle preparation and characterization are described in the Supporting Information.

The fluorescence quantum yields, Φ_{fl}, of PFBT nanoparticles and CdSe:ZnS quantum dots were measured using a fluorimeter with the samples exposed to ambient air, with the obtained results summarized in Table 1. Additional information on the fluorescence measurements is provided in the Supporting Information. The determined quantum yield of 0.41 for quantum dots is consistent with the literature.[16] While the undoped PFBT nanoparticles have a relatively low quantum yield (0.16), codoping with TPA and TSB increases the quantum yield by a factor of 2.4. We hypothesize that the antioxidant species donate electrons to the polymer, repairing existing oxidized defects (likely hole polarons), thus increasing fluorescence quantum yield.[17] Additionally, the dopants could disrupt polymer−polymer interactions, thus reducing aggregation-induced quenching. We did not observe leaching or loss of antioxidant, as photostability and quantum yield for particles stored several days were similar to those of freshly prepared particles. This result is in agreement with previous results, indicating negligible leaching of dyes incorporated in conjugated polymer nanoparticles.[15] However, it is likely that surfactants or other amphiphilic species could leach the antioxidants, as has been observed for hydrophobic dye dopants in conjugated polymer nanoparticles.[18]

The photobleaching kinetics of aqueous suspensions of particles were recorded with the samples exposed to air (Figure 2b) and analyzed to obtain the photobleaching quantum yield and estimated number of photons emitted per nanoparticle (Table 1), using the method of Rigler et al.[19] For additional information about the photostability measurements and analysis, see the Supporting Information. The addition of the antifade agents causes significant reduction in the rate of PFBT nanoparticle photobleaching and thus the quantum yield of photobleaching, Φ_{pb}. For instance, the Φ_{pb} of undoped PFBT nanoparticles is 5.6×10^{-9}, whereas that of the PFBT nanoparticles codoped with PASE and TSB decreases to 2.2

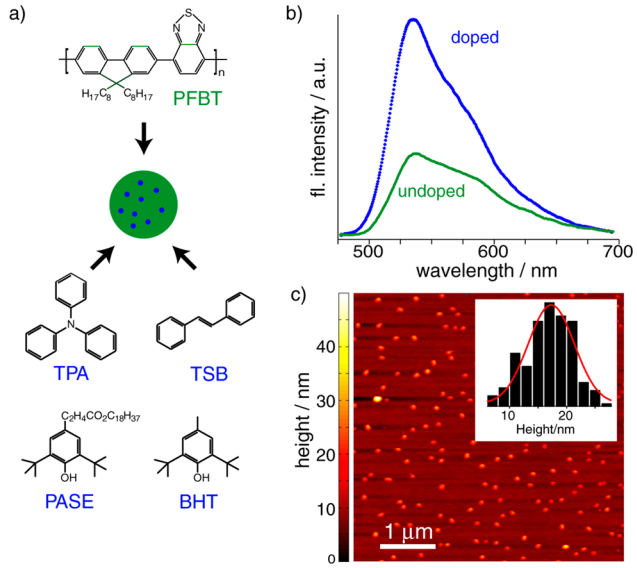

Figure 1. (a) Chemical structures of fluorescent conjugated polymer and four low-molecular-weight antifade agents employed. (b) Fluorescence emission spectra (λ_{ex} = 473 nm) of aqueous dispersions of the doped and undoped PFBT nanoparticles. (c) Typical AFM image of PFBT nanoparticles and histogram of particle height.

Table 1. Photostability and Brightness of PFBT Nanoparticles and CdSe:ZnS Quantum Dots, Ensemble Measurement

samples	Φ_{fl}	$\bar{\tau}_{pb}$	Φ_{pb}	photons (ensemble)
CdSe:ZnS QDs	0.41	3.7×10^4	1.0×10^{-7}	3.9×10^6
undoped PFBT NPs	0.16	1.4×10^4	5.6×10^{-9}	2.9×10^7
PASE/TSB-doped PFBT NPs	0.37	3.7×10^4	2.2×10^{-9}	1.7×10^8
TPA/TSB-doped PFBT NPs	0.38	3.8×10^4	2.1×10^{-9}	1.8×10^8
BHT/TSB-doped PFBT NPs	0.22	3.8×10^4	2.1×10^{-9}	1.0×10^8

dx.doi.org/10.1021/jp3086254 | J. Phys. Chem. B 2013, 117, 4517−4520

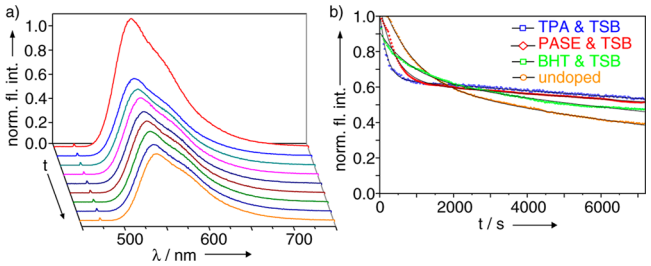

Figure 2. (a) Time evolution of fluorescence emission of TPA and TSB codoped PFBT nanoparticles (aqueous dispersion) upon continuous 473-nm laser illumination. Each spectrum contains a typical nanoparticle emission peak centered ~540 nm and a sharp scattered laser line at 473 nm. The elapsed time between each successive spectrum displayed is 900 s. (b) Comparison of the fluorescence decay kinetics curves of the doped and undoped PFBT nanoparticles (aqueous dispersion) upon continuous 473-nm laser irradiation.

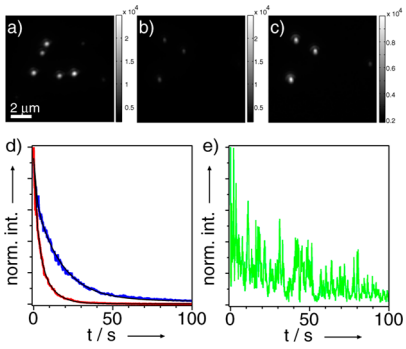

Figure 3. (a) Fluorescence microscopy images of PFBT nanoparticles codoped with PASE and TSB, gray scale ranging from 1800 (black) to 25000 (white). (b) Fluorescence microscopy images of undoped PFBT conjugated polymer nanoparticles using the same gray scale in panel a. (c) Same image as in panel b, with a gray scale ranging from 1800 to 10000. Images in panels a–c are acquired under identical conditions. This result indicates that the doped particles are roughly two times brighter than the undoped particles. (d) Comparison of the fluorescence decay curves of typical single doped (blue curve) and undoped (red curve) PFBT nanoparticles upon continuous 473-nm laser irradiation. (e) Fluorescence decay curves of a typical single quantum dot, under the same conditions as in panel d.

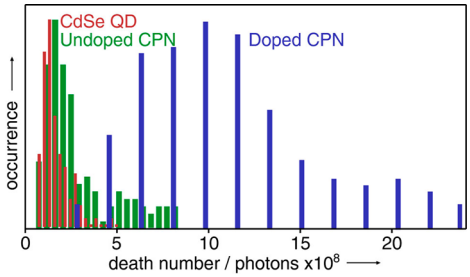

Figure 4. Comparison of death number (total number of photons emitted per single particle) histograms of CdSe:ZnS quantum dots (QD), undoped and doped PFBT conjugated polymer nanoparticles (CPNs). For each case, the histogram includes results from more than 150 individual nanoparticles.

$\times 10^{-9}$. The ratio Φ_{fl}/Φ_{pb} gives the average number of photons emitted per particle prior to photobleaching, a quantity referred to as the death number, N_{ave}.[19] The observed decrease in photobleaching quantum yield upon doping, together with the improvement of fluorescence quantum yield, leads to an overall enhancement of N_{ave} from 2.9×10^7 for undoped PFBT particles to 1.7×10^8 for particles codoped with PASE and TSB, an improvement of more than a factor of 5. Significantly, the addition of both PASE and TSB increases the death number more than either additive alone, perhaps since the PASE primarily acts to improve the fluorescence quantum yield, with some decrease in photobleaching quantum yield, while the TSB primarily acts to reduce the photobleaching quantum yield by triplet quenching.

We measured the single particle imaging and photobleaching kinetics of CdSe:ZnS quantum dots and PFBT conjugated polymer nanoparticles in air, using a fluorescence microscope equipped with a CCD detector. The methods are described in the Supporting Information. The improved fluorescence quantum yield of the doped PFBT nanoparticles is evident in the single particle fluorescence imaging, as shown in Figure 3. Additionally, the relative increase in fluorescence brightness upon doping observed at the single particle level is roughly consistent with that observed in ensemble fluorescence measurements. From analysis of the single particle fluorescence kinetics of PFBT nanoparticles and quantum dots (Figure 3), it can be seen that the antifade additives significantly decrease the rate of photobleaching, roughly doubling the lifetime. In contrast to the relatively smooth decay curves of PFBT nanoparticles, the fluorescence of single quantum dots exhibits pronounced photoblinking (Figure 3e), as previously reported.[20]

At the single molecule or particle level, a convenient measure of the photostability is the number of photons emitted per molecule or particle prior to photobleaching, N_{ave} (death number),[19] a quantity which can be obtained from fluorescence microscopy images by acquiring a sequence of images until the particles are nearly photobleached, and summing the signal for a given particle, factoring in the detection efficiency of the microscope and gain of the CCD. For each particle type (CdSe:ZnS quantum dots, undoped PFBT nanoparticles, and PFBT nanoparticles codoped with PASE and TSB), a histogram of the death numbers of more than 150 individual particles was generated (Figure 4). Not surprisingly, the presence of air significantly decreases the photostability of the undoped CPNs, with the average number of photons emitted per nanoparticle (1.8×10^8 photons) lower by more than 2 orders of magnitude than that previously reported for single particles under nitrogen protection.[6] The average number of photons emitted per individual doped PFBT CPN (1.1×10^9 photons) is more than 5 times that of the undoped PFBT CPNs, indicating that the combination of PASE and TSB greatly reduces the rate of photobleaching under single particle imaging conditions in air. However the rate of photobleaching is still significantly higher than that observed under nitrogen protection.[6] The somewhat higher death number for single particles as compared to the ensemble measurements of the same particles is attributable to differences in conditions; it is likely that the aqueous environment present in the ensemble experiments could be favorable for a number of free radical reactions involved in photobleaching. Nevertheless, both methods showed improvements in the death number by similar factors upon doping, indicating that the photostability improvement upon doping is robust. While quantum dots are widely reported to possess superior photostability as compared to other fluorophores, and there are qualitative comparisons to conventional fluorophores in the literature.[21] We are aware of

dx.doi.org/10.1021/jp3086254 | J. Phys. Chem. B 2013, 117, 4517–4520

no reports of quantitative ensemble photostability measurements of quantum dots in solution (e.g., photobleaching quantum yield) in the literature, and there is a single report of quantitative single quantum dot photostability measurements.[19] According to our measurements, the average number of photons emitted per doped PFBT CPN is approximately 7 times higher than that of the CdSe:ZnS quantum dots, under single particle imaging conditions.

CONCLUSION

In conclusion, we performed ensemble and single particle fluorescence measurements on conjugated polymer nanoparticles doped with various antifade agents, as a novel approach to obtain a better understanding of the photophysical and photochemical processes that dictate the brightness and photostability of conjugated polymer nanoparticles as well as possibly shedding light on processes that may also occur in conjugated polymer electro-optic devices. The results show that incorporation of antifade agents effectively improves the fluorescence quantum yield and photostability of the conjugated polymer nanoparticles, likely by a combination of triplet quenching and reduction of photogenerated hole polarons (cations), which act as fluorescence quenchers. The single particle results were in approximate agreement with the bulk results, providing some confirmation of the single particle approach for evaluating nanoparticle photostability. In addition, we quantitatively compared the photostability of conjugated polymer nanoparticles and CdSe quantum dots, at both the ensemble and single particle level, determining that doped conjugated polymer nanoparticles are significantly more photostable than CdSe quantum dots under the conditions employed. Furthermore, the observation that addition of antioxidants improves the fluorescence quantum yield of the particles lends support to the hypothesis that quenching by hole polarons can be a key factor in determining the luminescence efficiency of conjugated polymers. Additional investigations of these phenomena, by single particle fluorescence saturation measurements, and fluorescence lifetime measurements, are required to provide further support for this hypothesis and to provide additional details of the overall picture of relevant photophysical and photochemical processes, such as how the presence of antioxidants and triplet quenchers affects various rate constants.

ASSOCIATED CONTENT

Supporting Information

Detailed procedures of conjugated polymer nanoparticle preparation and characterization, fluorescence quantum yield and photobleaching quantum yield determination, and single particle photobleaching measurement. This material is available free of charge via the Internet at http://pubs.acs.org.

AUTHOR INFORMATION

Corresponding Author

*E-mail: mcneill@clemson.edu.

Notes

The authors declare no competing financial interest.

ACKNOWLEDGMENTS

J.D.M. and Z.Y.T. acknowledge financial support from the NSF under Grant No. CHE-1058885. Z.Y.T. thanks NSFC (Grant No. 21173262) for funding.

REFERENCES

(1) Yu, J. B.; Wu, C. F.; Sahu, S. P.; Fernando, L. P.; Szymanski, C.; McNeill, J. *J. Am. Chem. Soc.* **2009**, *131*, 18410−18414.
(2) Harbron, E. J.; Davis, C. M.; Campbell, J. K.; Allred, R. M.; Kovary, M. T.; Economou, N. J. *J. Phys. Chem. C* **2009**, *113*, 13707−13714.
(3) Wu, C. F.; Bull, B.; Christensen, K.; McNeill, J. *Angew. Chem., Int. Ed.* **2009**, *48*, 2741−2745.
(4) Kaeser, A.; Schenning, A. P. H. J. *Adv. Mater.* **2010**, *22*, 2985.
(5) Wu, C. F.; Schneider, T.; Zeigler, M.; Yu, J. B.; Schiro, P. G.; Burnham, D. R.; McNeill, J. D.; Chiu, D. T. *J. Am. Chem. Soc.* **2010**, *132*, 15410−15417.
(6) Wu, C. F.; Bull, B.; Szymanski, C.; Christensen, K.; McNeill, J. *ACS Nano* **2008**, *2*, 2415−2423.
(7) Sivaguru, J.; Solomon, M. R.; Poon, T.; Jockusch, S.; Bosio, S. G.; Adam, W.; Turro, N. J. *Acc. Chem. Res.* **2008**, *41*, 387−400.
(8) Longin, A.; Souchier, C.; French, M.; Bryon, P. A. *J. Histochem. Cytochem.* **1993**, *41*, 1833−1840.
(9) Scherf, U.; List, E. J. W. *Adv. Mater.* **2002**, *14*, 477−487.
(10) Abbel, R.; Woffs, M.; Bovee, R. A. A.; van Dongen, J. L. J.; Lou, X.; Henze, O.; Feast, W. J.; Meijer, E. W.; Schenning, A. P. H. J. *Adv. Mater.* **2009**, *21*, 597−602.
(11) Andrew, T. L.; Swager, T. M. *Macromolecules* **2008**, *41*, 8306−8308.
(12) Tian, Z. Y.; Yu, J. B.; Wu, C. F.; Szymanski, C.; McNeill, J. *Nanoscale* **2010**, *2*, 1999−2011.
(13) Yu, J. B.; Wu, C. F.; Tian, Z. Y.; McNeill, J. *Nano Lett.* **2012**, *12*, 1300−1306.
(14) Szymanski, C.; Wu, C. F.; Hooper, J.; Salazar, M. A.; Perdomo, A.; Dukes, A.; McNeill, J. *J. Phys. Chem. B* **2005**, *109*, 8543−8546.
(15) Wu, C. F.; Zheng, Y. L.; Szymanski, C.; McNeill, J. *J. Phys. Chem. C* **2008**, *112*, 1772−1781.
(16) Lounis, B.; Bechtel, H. A.; Gerion, D.; Alivisatos, P.; Moerner, W. E. *Chem. Phys. Lett.* **2000**, *329*, 399−404.
(17) Deussen, M.; Bolivar, P. H.; Wegmann, G.; Kurz, H.; Bassler, H. *Chem. Phys.* **1996**, *207*, 147−157.
(18) Yu, J. B.; Wu, C. F.; Zhang, X.; Fangmao, Y.; Gallina, M. E.; Rong, Y.; Wu, I. C.; Sun, W.; Chan, Y. H.; Chiu, D. T. *Adv. Mater.* **2012**, *24*, 3498−3504.
(19) Eggeling, C.; Widengren, J.; Rigler, R.; Seidel, C. A. M. *Anal. Chem.* **1998**, *70*, 2651−2659.
(20) Nirmal, M.; Dabbousi, B. O.; Bawendi, M. G.; Macklin, J. J.; Trautman, J. K.; Harris, T. D.; Brus, L. E. *Nature* **1996**, *383*, 802−804.
(21) Michalet, X.; Pinaud, F.; Lacoste, T. D.; Dahan, M.; Bruchez, M. P.; Alivisatos, A. P.; Weiss, S. *Single Mol.* **2001**, *2*, 261−276.